Dyes and Pigments 182 (2020) 108697

Contents lists available at ScienceDirect

Dyes and Pigments

journal homepage: http://www.elsevier.com/locate/dyepig

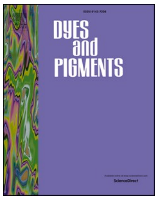

Dibenzothiophene dioxide-benzofuro carbazole based bipolar host material for yellow and red phosphorescent OLEDs

Hee Jung Jang [a,1], Ramanaskanda Braveenth [a,1], Kanthasamy Raagulan [a], Seung Yu Choi [a], Young Hee Park [a], Su Bin Oh [a], Il-Ji Bae [b], Bo Mi Kim [c], Qiong Wu [d,**], Miyoung Kim [b,***], Kyu Yun Chai [a,*]

[a] *Division of Bio-Nanochemistry, College of Natural Sciences, Wonkwang University, Iksan City, Chonbuk, 570-749, Republic of Korea*
[b] *Nano-Convergence Research Center, Korea Electronics Technology Institute, Jeonju, Republic of Korea*
[c] *Department of Chemical Engineering, Wonkwang University, Iksan, 570-749, Republic of Korea*
[d] *Department of Chemistry and Chemical Engineering, Hebei Normal University for Nationalities, Chengde, 067-000, PR China*

ARTICLE INFO

Keywords:
Organic light emitting diodes
Benzofuro carbazole
Bipolar host
Dibenzothiophene dioxide

ABSTRACT

2-(12H-benzofuro[3,2-*a*]carbazol-12-yl)dibenzo[b,d]thiophene 5,5-dioxide (DBT-INFUR) is a bipolar host material for yellow and red phosphorescent OLEDs. DBT-INFUR was designed and synthesized between dibenzothiphene acceptor and benzofuro carbazole donor with a yield of 60%. We constructed two different devices, namely a yellow and a red phosphorescent OLEDs, and we compared the device properties with reference 4,4′-Bis (N-carbazolyl)-1,1′-biphenyl (CBP). DBT-INFUR based yellow phosphorescent OLED device exhibited maximum current and external quantum efficiencies of 41.07 cd/A and 16.5%, respectively and which is better than that of reference CBP based similar device (27.66 cd A, 10.15%). DBT-INFUR based red phosphorescent OLED (12.44%) revealed higher efficiencies when compared to the reference (7.64%) device. The bipolar DBT-INFUR showed excellent host properties with yellow and red phosphorescent devices.

1. Introduction

Over the past few decades, organic optoelectronic devices have developed rapidly in terms of both device fabrication techniques and materials design. Especially, organic light emitting diodes (OLEDs) have shown prominent growth in commercial markets in the form of television, mobile phones and lighting sources [1,2]. OLEDs exhibited good advantages, such as low power consumption, wide view angle, high brightness, color purity and possibility of fabrication in various substrates [3–5]. The first-generation OLEDs used only fluorescent dopants, which expressed low internal quantum efficiency (IQE) of 25% with only chance of singlet emission. The IQE of 100% were achieved first time when a heavy metal based second generation dopant was employed. Which metal-ligand complex helped to harvest both singlet and triplet excitons through inter system crossing (ISC) mechanism. Phosphorescent OLEDs posses' major disadvantages of expensive noble metal complexes employed as dopant, so the third-generation metal free fluorescent dopants were introduced, and which is known as thermally activated delayed fluorescence (TADF) OLEDs. Metal free dopants showed 100% IQEs with fluorescence emission through the mechanism of reverse inter system crossing (RISC) [6–19].

Phosphorescent OLEDs received much attention due to its high color purity and considerable device efficiencies. The emission layer of phosphorescent OLEDs consists of host and dopant materials [20–22]. Host-dopant combination suppress the acute triplet exciton polaron quenching, concentration quenching and triplet-triplet annihilation [23–28]. Host materials are major energy suppliers to the dopant material while maintaining the charge balance at emission layer [21]. There are three types of host materials have been identified, which are hole transport type, electron transport type and bipolar host materials [29–34]. Hole transporting (HT) host materials build with electron donating carbazole and diphenylamine units. 4,4′-Bis(N-carbazolyl)-1,

---

* Corresponding author.
** Corresponding author.
*** Corresponding author.
E-mail addresses: wuqiong9308@126.com (Q. Wu), miy1kim@keti.re.kr (M. Kim), geuyoon@wonkwang.ac.kr (K.Y. Chai).
[1] These authors contributed equally to this work.

https://doi.org/10.1016/j.dyepig.2020.108697
Received 21 February 2020; Received in revised form 16 May 2020; Accepted 4 July 2020
Available online 20 July 2020

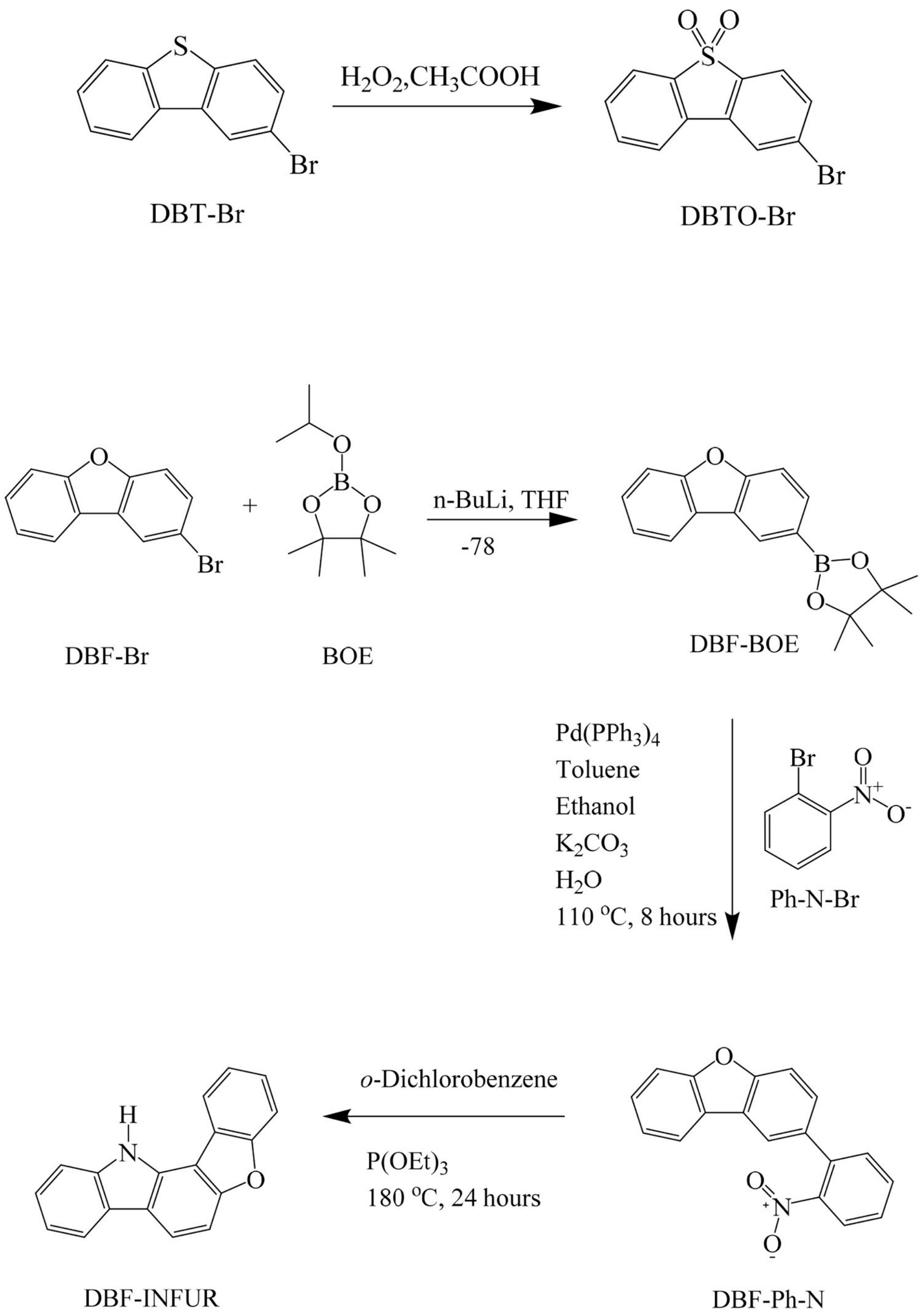

Scheme 1. Synthetic scheme of starting materials **DBTO-Br** and **DBF-INFUR**.

1′-biphenyl (CBP), 1,3-Bis(N-carbazolyl)benzene (mCP) and 3,3-Di (9H-carbazol-9-yl)biphenyl (mCBP) are well-known hole transporting type host materials [11,35–44]. Bis[2-(diphenylphosphino)phenyl] ether oxide (DPEPO), dibenzo[b,d]furan-2,8-diylbis(diphenylphosphine oxide) (DBFPO) and 8-Hydroxyquinoline aluminum salt (Alq_3) are identified best electron transport type (ET) host materials for phosphorescent and TADF OLEDs [45–49]. Moreover, pure hydrocarbon-based design strategy proposed in OLED applications. Especially, 9,9′-spirobifluorene (SBF) based moieties were studies with certain modifications at substituent positions. which also showed better device performances with red, green, and blue phosphorescent OLEDs [50,51].

The ET and HT type host materials showed several drawbacks, such as low thermal stabilities, recombination occurs towards either electron transport layer or hole transport layer and imbalanced charges at emission layer [52,53]. Additionally, phosphorescence emitters show longer excited lifetime, self-quenching, and triplet polaron quenching at high concentration, which lead to poor electroluminescent performances. To overcome these issues, bipolar host materials were identified with both electron donating (p type) and electron withdrawing (n type) moieties present in a single molecule. The bipolar host materials brought an interesting feature, such as broad charge recombination zone, well balanced holes and electrons, thermal stabilities and well-matched frontier molecular orbital (FMO) energies with adjacent layers [54–59]. Additionally, one of the most key factors for a host material is triplet energy. Host material should own higher triplet energy than the dopant material to prevent the energy flow back [60–62]. A suitable molecular design can fulfill the demands in order to enhance the device efficiencies [63]. In our previous work, we designed a bipolar molecule

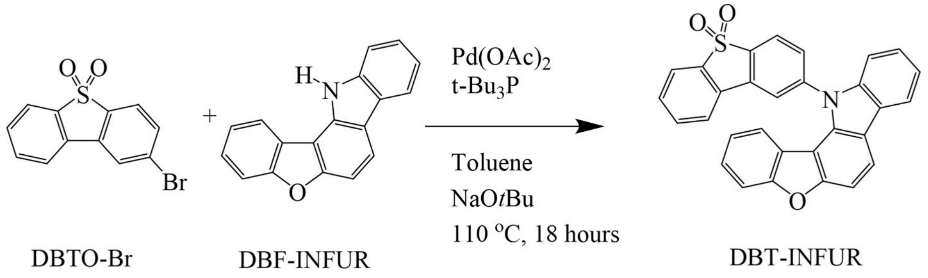

Scheme 2. Synthetic route of target bipolar material **DBT-INFUR**.

DBTO-IN/CAR between dibenzothiophene oxide acceptor and indolocarbazole donor. Green phosphorescent OLED device with DBTO-IN/CAR as host revealed excellent current and external quantum efficiencies of 51.98 cd/A and 19.03%, respectively [53].

In this work, we designed and synthesized dibenzothiophene oxide-benzofuro carbazole based bipolar host material 2-(12H-benzofuro[3,2-a]carbazol-12-yl)dibenzo[b,d]thiophene 5,5-dioxide (DBT-INFUR). The synthetic methods are shown in Scheme 1 and Scheme 2. Two different OLED devices were fabricated with yellow and red phosphorescent dopants to investigate the device properties. Iridium(III) bis(4-(4-tert-butylphenyl) thieno[3,2-c]pyridinato-N,C2′) acetylacetonate (PO-01-TB) and Bis[2-(3,5-dimethylphenyl)-4-methyl -quinoline](acetylacetonate)iridium(III) (Ir(mphmq)$_2$(acac)) were applied as yellow and red phosphorescent, respectively. We can expect good device performances from yellow and red phosphorescent devices when compare to the reference CBP host material.

2. Experimental details

2.1. Synthesis of 2-bromodibenzothiophene 5,5-dioxide (DBTO-Br)

A mixture of 2-bromodibenzothiophene (**DBT-Br**, 4.0 g, 15 mmol) and acetic acid (**AcOH**, 200 ml) was refluxed at 60 °C for 30 min while stirring in a two-neck round-bottom flask equipped with a condenser. After 30 min, 30% of hydrogen peroxide (**H_2O_2**, 100 ml) was dropped to the reaction mixture. The reaction mixture was stirred at 80 °C for a further 2 h. Then, a white precipitate was filtered and washed with deionized water several times and dried to obtain 3.8 g of the dried product **DBTO-Br**.

Yield: 85%; White solid; ^{1}H NMR (500 MHz, $CDCl_3$) δ 7.92 (S, 1H), 7.82–7.83 (d, *J* = 8 Hz, 1H), 7.75–7.76 (d, *J* = 8 Hz, 1H), 7.64–7.69 (m, 3H), 7.54–7.57 (t, *J* = 7.5, 1H); ^{13}C NMR (500 MHz, $CDCl_3$) δ 138.1, 136.5, 134.1, 133.6, 133.3, 131.1, 130.3, 128.7, 125.0, 123.5, 122.4, 121.8.

2.2. Synthesis of 2-(dibenzo[b,d]furan-2-yl)-4,4,5,5-tetramethyl-1,3,2-dioxaborolane (DBF-BOE)

2-bromodibenzo[b,d]furan (**DBF-Br**, 5 g, 20.24 mmol) was vacuumed for 15 min in a 250 ml round bottom flask. Anhydrous THF of 150 ml was added under inner condition, and mixture was kept stirring under −78 °C for 30 min. Then *n*-BuLi (2.5 M, 12.5 ml) was injected drop wisely, and mixture kept stirring under the same temperature. After 1 h, 2-isopropoxy-4,4,5,5-tetramethyl-1,3,2-dioxaborolane (**BOE**, 7.5 ml, 36.76 mmol) was added slowly, and the reaction mixture kept overnight to brought room temperature. The work up was held three times by using deionized water and dichloromethane. Organic layer was dried over anhydrous $MgSO_4$, filtered and concentrated through rotary evaporator. A silica column with *n*-Hexane: dichloromethane solvent system used to obtain 5 g of the **DBTO-BOE.**

Yield: 84%; Colorless oil; ^{1}H NMR (500 MHz, $CDCl_3$) δ 8.45 (S, 1H), 7.96–7.97 (d, *J* = 8.5 Hz, 1H), 7.92–7.94 (dd, *J* = 8.5, 1.5 Hz, 1H), 7.55–7.57 (d, *J* = 8.5 Hz, 2H), 7.43–7.46 (m, 1H), 7.33–7.36 (m, 1H), 1.39 (s, 12H).

2.3. Synthesis of 2-(2-nitrophenyl)dibenzo[b,d]furan (DBF-Ph-N)

A mixture of 2-(dibenzo[b,d]furan-2-yl)-4,4,5,5-tetramethyl-1,3,2-dioxaborolane (**DBF-BOE**, 6.5 g, 22.09 mmol), 1-bromo-2-nitrobenzene (**Ph-N-Br**, 4.91 g, 24.30 mmol), catalyst (**$Pd(PPh_3)_4$**, 0.77 g, 0.66 mmol), 2 M K_2CO_3 (13.82 g, 100 mmol), deionized water (50 ml), ethanol (30 ml) and toluene (100 ml) were refluxed at 110 °C for 8 h while stirring. After completion of the reaction, mixture was work worked up by using deionized water and dichloromethane. Organic layers were dried and evaporated. The crude mixture was separated by silica column chromatography (*n*-Hexane and dichloromethane) to obtain 6 g of **DBF-Ph-N.**

Yield: 94%; Yellow solid; ^{1}H NMR (500 MHz, $CDCl_3$) δ 7.93–7.94 (d, *J* = 7.5 Hz, 1H), 7.88–7.90 (m, 2H), 7.58–7.66 (m, 3H), 7.46–7.54 (m, 3H), 7.34–7.39 (m, 2H).

2.4. Synthesis of 12H-benzofuro[3,2-a]carbazole (DBF-INFUR)

A mixture of 2-(2-nitrophenyl)dibenzo[b,d]furan (**DBF-Ph-N**, 6g, 20.76 mmol), triethyl phospite (**$P(OEt)_3$**, 70 ml) and *o*-dichlorobenzene (70 ml) was refluxed at 180 °C for 24 h under inert condition. After completion of the reaction, reaction mixture was concentrated, and crude mixture was separated by using silica column (*n*-Hexane and dichloromethane).

Yield: 75%; Pale white solid; ^{1}H NMR (500 MHz, $CDCl_3$) δ 8.55 (S, 1H), 8.14–8.16 (d, *J* = 8.5 Hz, 1H), 8.11–8.13 (d, *J* = 8 Hz, 1H), 8.06–8.08 (d, *J* = 8 Hz, 1H), 7.66–7.67 (d, *J* = 8 Hz, 1H), 7.58–7.60 (d, *J* = 8 Hz, 1H) 7.42–7.51 (m, 5H), 7.30–7.33 (t, *J* = 7.5 Hz, 1H).

2.5. Synthesis of 2-(12H-benzofuro[3,2-a]carbazol-12-yl)dibenzo[b,d] thiophene 5,5-dioxide (DBT-INFUR)

A mixture of 2-bromodibenzothiophene 5,5-dioxide (**DBTO-Br**, 1.0 g, 3.38 mmol), 12H-benzofuro[3,2-a]carbazole (**DBF-INFUR**, 1.0 g, 3.88 mmol), Pd(OAc)$_2$ (0.05 g, 0.20 mmol), 10% *t*-Bu$_3$P in toluene (0.98 ml, 4.06 mmol), NaO*t*Bu (1.0 g, 10.40 mmol) and 80 ml of anhydrous toluene was added in a two-neck round-bottom flask equipped with a condenser. The mixture refluxed at 110 °C for 18 h inert atmosphere while stirring. The crude residues were separated by a silica column and *n*-hexane- dichloromethane solvent system to obtain the target molecule **DBT-INFUR** of 0.96g.

Yield: 60%; Pale yellow solid; ^{1}H NMR (500 MHz, $CDCl_3$) δ 8.25–8.27 (d, *J* = 8.5 Hz, 1H), 8.18–8.19 (d, *J* = 7.5 Hz, 1H), 8.11–8.13 (d, *J* = 8 Hz, 1H), 7.96 (s, 1H), 7.91–7.93 (m, 1H), 7.75–7.77 (d, *J* = 7.5 Hz, 1H), 7.55–7.64 (m, 4H), 7.37–7.44 (m, 3H), 7.25–7.31 (m, 1H), 6.92–6.95 (t, *J* = 7.5 Hz, 1H), 6.03–6.04 (d, *J* = 8 Hz, 1H)); ^{13}C NMR (500 MHz, $CDCl_3$) δ 156.7, 155.8, 144.8, 141.4, 138.4, 137.3, 135.4, 134.2, 134.0, 131.3, 130.6, 130.5, 126.3, 125.6, 124.5, 124.0, 122.8, 122.7, 122.5, 122.1, 121.8, 121.6, 120.0, 119.8, 119.6, 11.4, 109.9, 109.0, 105.8. MS (APCI) *m/z*: 472.28 for $C_{30}H_{17}NO_3S$ $[(M + H)^+]$; MS (TOF) *m/z*: 471.0929 for $C_{30}H_{17}NO_3S$ (471.0929); Anal. Calcd for

Table 1
Physical properties of **DBT-INFUR**.

HOST	T_m[a] (°C)	T_d[b] (°C)	UV–Vis[c] (nm)	PL max[d] (nm)	HOMO[e] (eV)	LUMO[f] (eV)	E_g[g] (eV)	E_T[h] (eV)
DBT-INFUR	236	371	297, 327 341	460[i] 457[j]	−5.87	−2.61	3.26	2.71

[a] Melting point.
[b] Thermal decomposition temperature.
[c] UV absorption wavelength in toluene.
[d] Photoluminescent maximum emission in THF.
[e] Highest occupied molecular orbital energy.
[f] Lowest unoccupied molecular orbital energy.
[g] Energy band gap.
[h] Triplet energy.
[i] Room temperature.
[j] Low temperature.

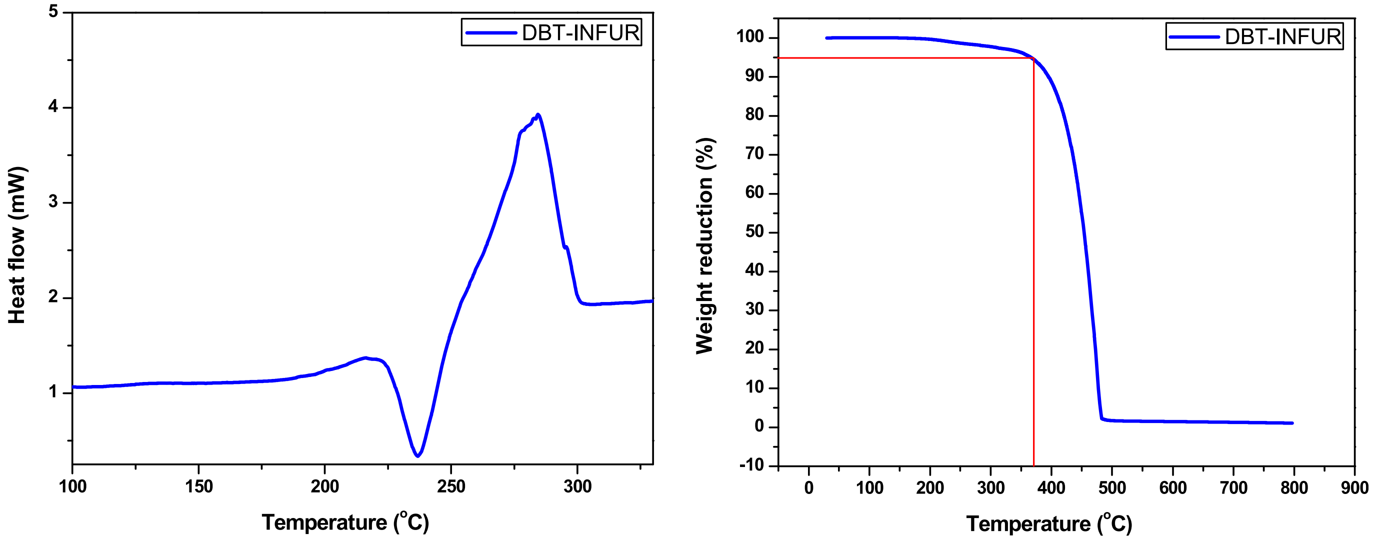

Fig. 1. Differential scanning calorimetry and thermal gravimetric analysis of **DBT-INFUR**.

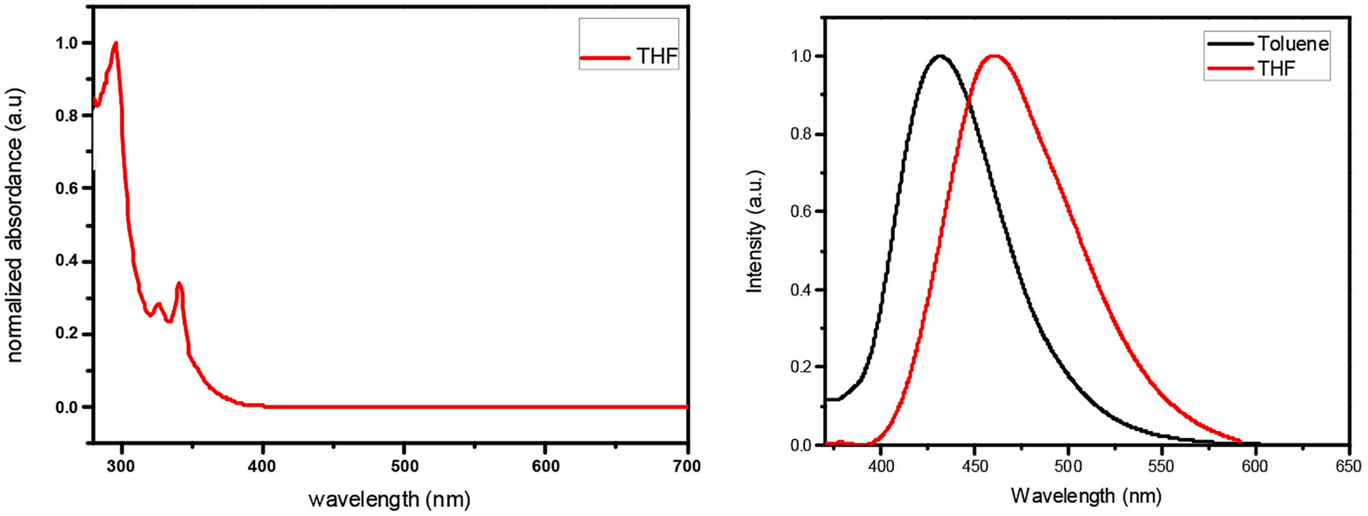

Fig. 2. UV–Vis absorption and photoluminescent spectra of **DBT-INFUR**.

$C_{30}H_{17}NO_3S$ (%): C, 76.42; H, 3.63; N, 2.97; O, 10.18; S, 6.80. Found: C, 75.32; H, 3.62; N, 3.05; O, 9.97; S, 6.51.

3. Results and discussion

The thermal properties of DBT-INFUR were studied by thermo gravimetric analysis (TGA) and differential scanning calorimetry (DSC) under nitrogen atmosphere with the heating rate of 10 °C per minute. All

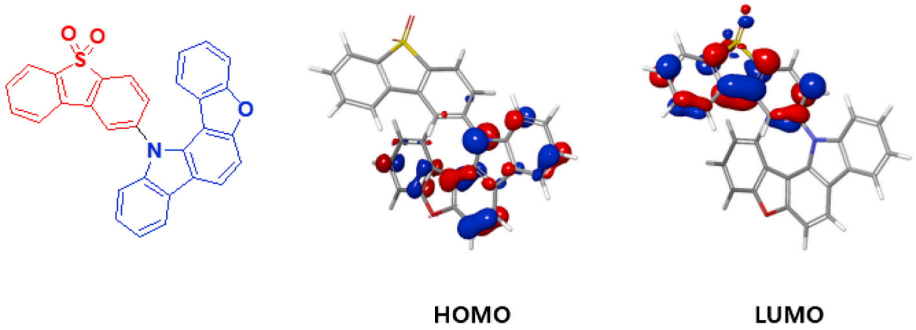

Fig. 3. Frontier molecular orbital distribution of **DBT-INFUR**.

Table 2
Calculation data of **DBT-INFUR**.

Calculation data of DBT-INFUR					
Optical properties			Electrochemical properties		
T_1 (eV)	S_1 (eV)	ΔE_{st} (eV)	HOMO (eV)	LUMO (eV)	Band gap (eV)
2.929	3.086	0.157	5.97	2.93	3.03

data are summarized in Table 1 and depicted in Fig. 1. The thermal decomposition of our material was observed at 371 °C for a 10% weight reduction, and the melting point was noticed at 236 °C. These properties can help the morphological stabilities of the device.

The UV–vis absorption and photoluminescent spectra are depicted in Fig. 2 and summarized in Table 1. The UV absorption peaks were observed at 297, 327 and 342 nm, respectively in toluene solvent. The short wavelength absorption about 297 nm corresponding to π– π* transition of benzofuro carbazole moiety. The weaker absorption at long wavelength around 327 nm attributed to n–π* transition. The band gap energy of 3.26 eV was observed and which is almost similar with that of indolocarbazole based DBTO-IN/CAR molecule [51]. The charge transfer absorption from the benzofuro carbazole to dibenzothiophene oxide was noticed at 342 nm. The maximum photoluminescent emission was found at 431 and 460 nm in toluene and THF solvents, respectively. The low temperature (77K) photoluminescent emission was recorded at 457 nm, and the triplet energy was calculated as 2.71 eV. The triplet energy in toluene was calculated as 2.53 eV. The triplet energy is one of the important parameters for a device to prevent the energy flow back from the dopant material. Thus, we believe DBT-INFUR will support a great efficiency enhancement in yellow and red phosphorescent OLED

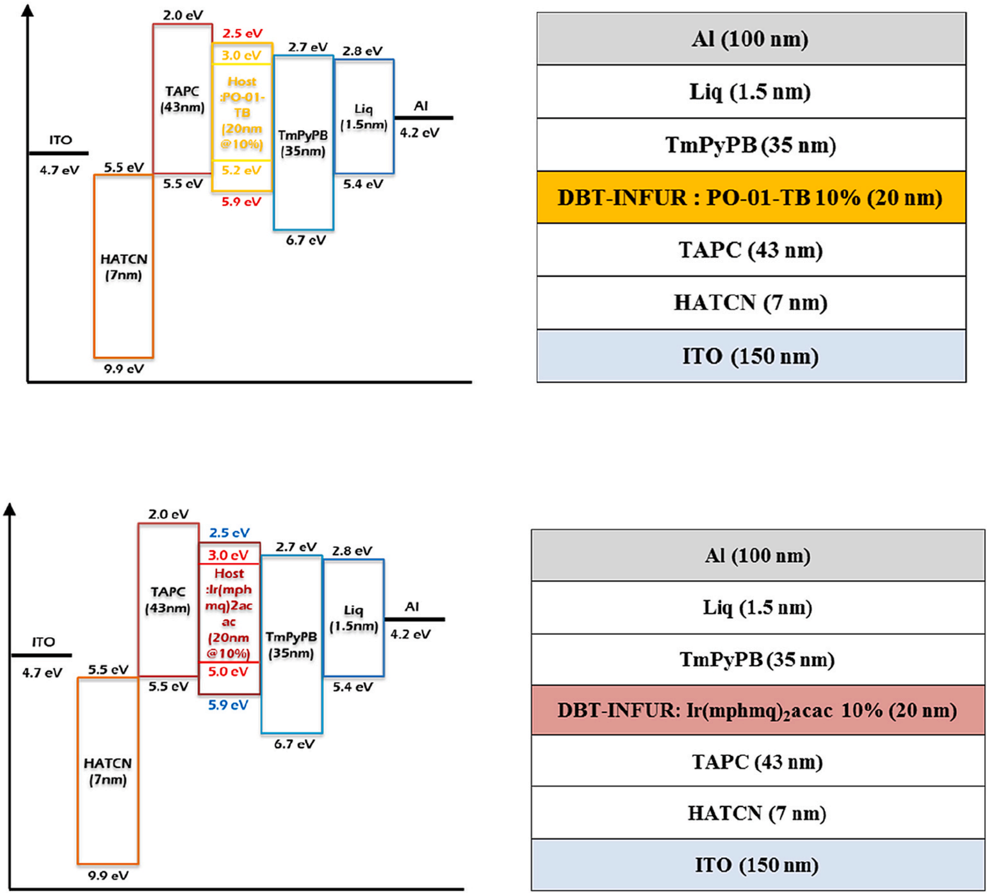

Fig. 4. Device structure of yellow and red phosphorescent OLEDs. (For interpretation of the references to color in this figure legend, the reader is referred to the Web version of this article.)

Table 3
Device characteristics of **DBT-INFUR** based yellow and red phosphorescent OLEDs compare with reference **CBP**.

Device characteristics	Reference CBP (Yellow device)	DBT-INFUR (Yellow device)	Reference CBP (Red device)	DBT-INFUR (Red device)
Turn-on voltage (V)	5.5	6.0	6.0	5.5
Current Efficiency (cd/A)	27.66	41.07	8.73	15.49
Power Efficiency (lm/W)	15.80	21.50	4.57	8.85
EQE (%)	10.15	16.50	7.64	12.44
CIE (x,y)	0.48, 0.50	0.49, 0.48	0.63,0.35	0.64, 0.35

devices.

The highest occupied molecular orbital (HOMO) energy level was obtained as −5.87 eV and which was achieved using the AC2 photoelectron spectrometer. The lowest unoccupied molecular orbital (LUMO) energy was calculated by adding the band gap value to the HOMO energy level, and which was −2.61 eV (Table 1). To investigate the molecular orbital distribution, we performed basic density functional theory DFT with a basic set of 6-31G using a Gaussian 09 [47]. The frontier molecular orbital distributions are depicted in Fig. 3. The LUMO distribution noticed over the electron withdrawing dibenzothiophene oxide moiety, while HOMO distribution was over the electron donating benzofuro carbazole unit. The dihedral angle between donor and acceptor was calculated as 64°. But we observed a small overlapping over the aromatic ring in dibenzothiophene oxide moiety, and which increases the energy difference between excited singlet and triplet states (0.15 eV). The calculation data are summarized in Table 2.

To investigate the electroluminescent properties of our bipolar host material DBT-INFUR, various phosphorescent OLED devices were fabricated with red and yellow phosphorescent dopants. The yellow and red device structures were as follow: indium tin oxide (ITO) (150 nm)/ 1,4,5,8,9,11-Hexaazatriphenylenehexacarbonitrile (HATCN) (7 nm)/ 4,4′-Cyclohexylidenebis[N,N-bis(4-methylphenyl)benzenamine](TAPC) (43 nm)/DBT-INFUR: 10 wt% Iridium(III) bis(4-(4-tert-butylphenyl) thieno[3,2-c]pyridinato-N,C2′) acetylacetonate (PO–O1) or Bis[2-(3,5-dimethylphenyl)-4-methyl -quinoline](acetylace tonate)iridium(III) (Ir (mphmq)$_2$(acac)) (20 nm)//1,3,5-Tri(m-pyridin-3-ylphenyl)benzene

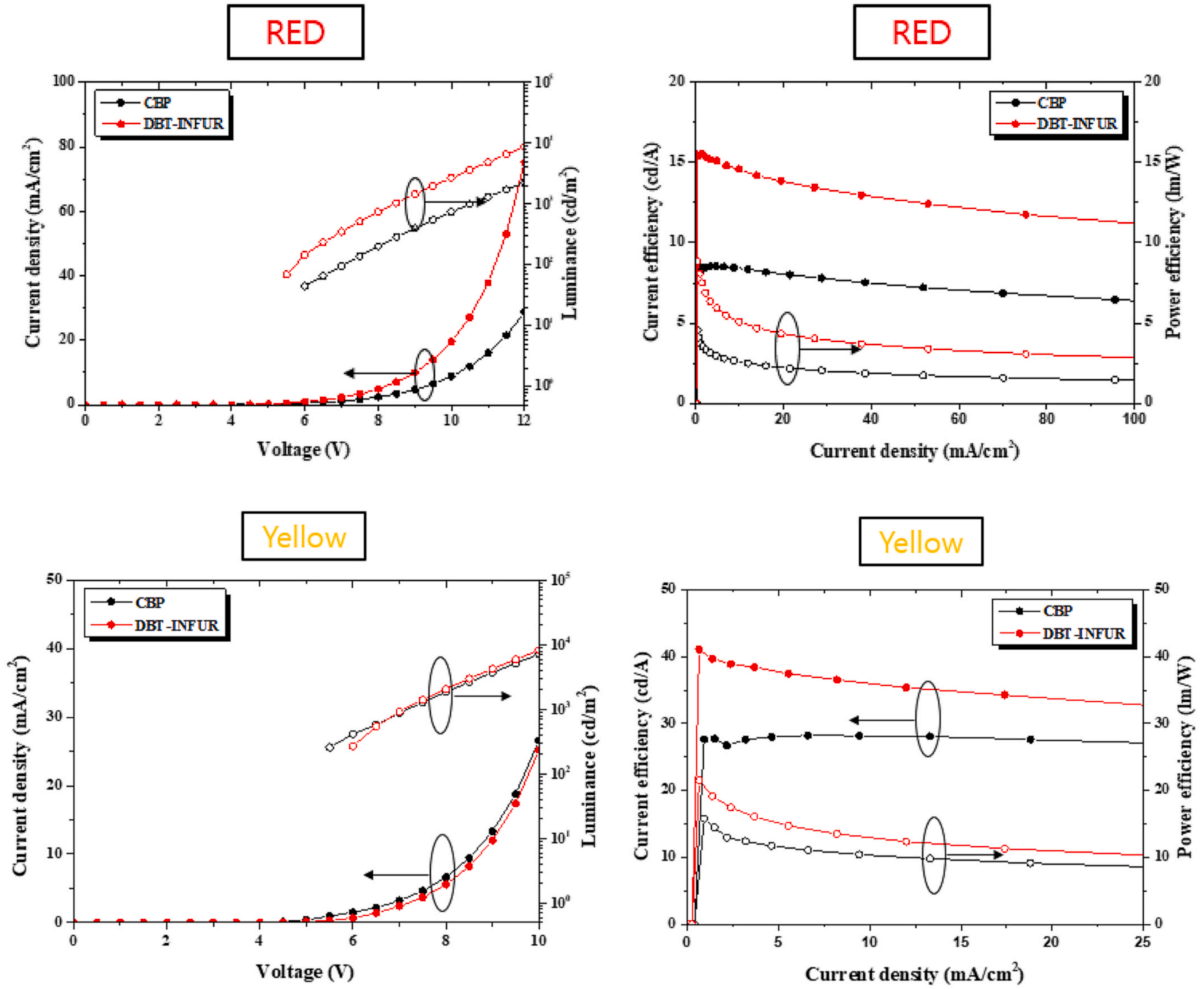

Fig. 5. Current density-voltage and luminescence-voltage of red and yellow phosphorescent OLEDs. (For interpretation of the references to color in this figure legend, the reader is referred to the Web version of this article.)

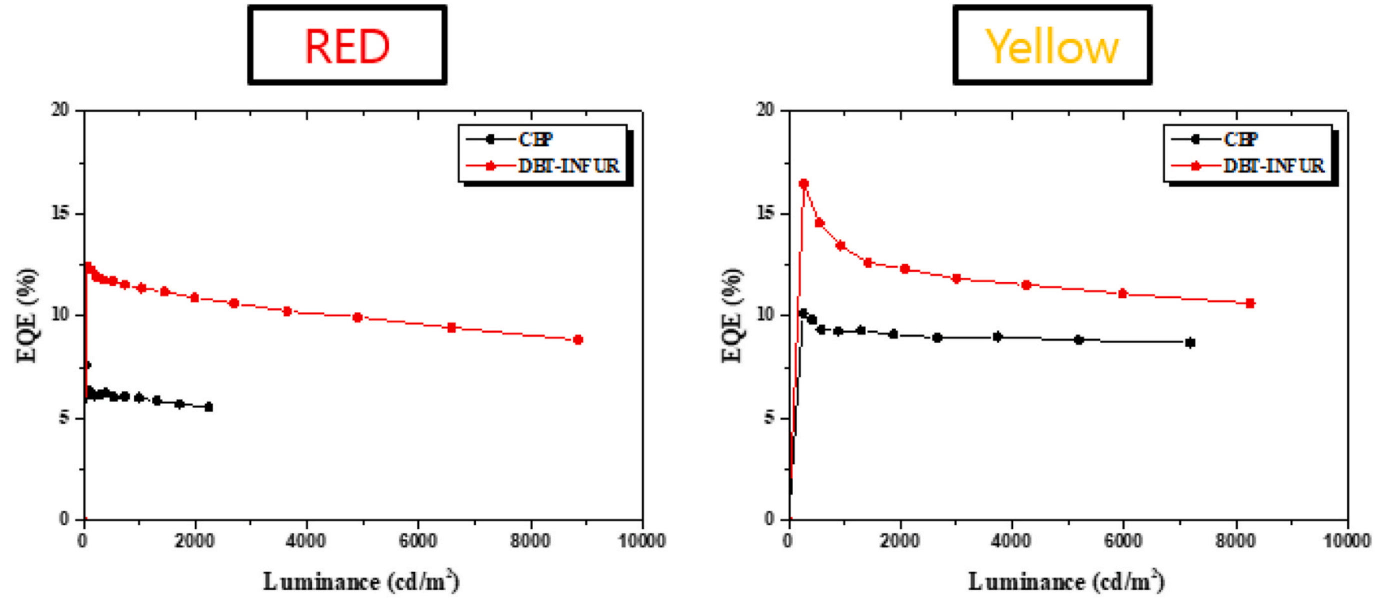

Fig. 6. External quantum efficiencies of yellow and red phosphorescent OLEDs. (For interpretation of the references to color in this figure legend, the reader is referred to the Web version of this article.)

(TmPyPB) (35 nm)/8-Quinolinolato lithium (Liq) (1.5 nm)/Aluminum (Al) (100 nm. ITO used for anode while cathode was Al, HATCN used as hole injecting layer (HIL), Liq for the electron injecting layer (EIL) and TAPC as the hole transporting layer (HTL) while TmPyPB employed as electron transport layer (ETL). Yellow and red phosphorescent dopants were PO-O1 and Ir(mphmq)$_2$(acac), respectively. Both yellow and red phosphorescent OLED properties were compared with reference 4,4′-Bis (N-carbazolyl)-1,1′-biphenyl (CBP) material in a similar structure. The device structures and energy diagrams are depicted in Fig. 4.

The current density-voltage-luminescence performances of yellow and red phosphorescent OLEDs are summarized in Table 3 and showed in Figs. 5 and 6. Bipolar host DBT-INFUR based device showed higher turn on voltage of 6 V when compared to reference device (5.5 V). But the driving voltage of both devices were same as 7 V. The current efficiency of yellow phosphorescent devices based on DBT-INFUR and CBP was 41.07 and 27.66 cd/A, respectively. Moreover, power efficiency of DBT-INFUR and CBP based yellow devices was 21.50 and 15.80 lm/W, which explains that our bipolar material exhibited higher efficiencies due its bipolar nature. The DBT-INFUR based yellow OLED devices showed higher external quantum efficiencies of 16.50%, which is better than that of reference device (10.15%). The red phosphorescent OLEDs with DBT-INFUR revealed excellent device efficiencies of 15.49 cd/A and 12.44% for current and external quantum efficiency, respectively. The reference device with CBP host materials showed lower device performances (8.73 cd/A and 7.64%).

Our bipolar host material DBT-INFUR exhibited excellent device efficiencies with both yellow and red phosphorescent OLEDs. The bipolar nature of DBT-INFUR enhanced the device efficiencies while maintain a proper charge balance at the emission layer. The CIE color coordinates (x,y) were (0.49, 0.48) and (0.64, 0.35) for yellow and red phosphorescent devices, respectively.

4. Conclusion

A bipolar host material DBT-INFUR material was designed and synthesized using a dibenzothiophene dioxide-benzofuro carbazole moieties. Yellow phosphorescent OLEDs with our bipolar host material exhibited excellent current, power and external quantum efficiencies of 41.07 cd/A, 21.50 lm/W and 16.50%, respectively. Which is much higher than that of the CBP-based reference device (27.66 cd/A, 15.80 lm/W and 10.15%). The external quantum efficiencies of red phosphorescent OLEDs were 12.44 and 7.64% for DBT-INFUR and reference CBP-based devices, respectively. DBT-INFUR bipolar host materials reveled excellent device performances with both yellow and red phosphorescent OLEDs while compare to the reference CBP- based similar devices. DBT-INFUR is a potential host candidate to enhance the efficiencies in yellow and red phosphorescent OLEDs.

Declaration of competing interest

The authors declare that they have no known competing financial interests or personal relationships that could have appeared to influence the work reported in this paper.

CRediT authorship contribution statement

Hee Jung Jang: Methodology. **Ramanaskanda Braveenth:** Conceptualization, Software, Investigation, Writing - original draft, Writing - review & editing. **Kanthasamy Raagulan:** Data curation. **Seung Yu Choi:** Methodology. **Young Hee Park:** Methodology. **Su Bin Oh:** Software. **Il-Ji Bae:** Formal analysis, Data curation. **Bo Mi Kim:** Resources, Funding acquisition. **Qiong Wu:** Investigation. **Miyoung Kim:** Formal analysis. **Kyu Yun Chai:** Conceptualization, Resources, Project administration, Funding acquisition.

Acknowledgement

This research was supported by the Basic Science Research Program through the National Research Foundation of Korea (NRF), funded by the education (NRF-2016R1D1A3B01015531) and also this work was supported by the National Research Foundation of Korea Grant funded by the Korean Government (NRF-2017R1C1B5076425). Authors thank Hebei Education Department Science Foundation (NO. QN2018313) and Science Foundation of Hebei Normal University for Nationalities (NO. 2018005) for their support.

Appendix A. Supplementary data

Supplementary data related to this article can be found at https://doi.org/10.1016/j.dyepig.2020.108697.

References

[1] Fröbel M, Fries F, Schwab T, Lenk S, Leo K, Gather MC, et al. Three-terminal RGB full-color OLED pixels for ultrahigh density displays. Sci Rep 2018;8(1):9684.
[2] Ito T, Sasabe H, Nagai Y, Watanabe Y, Onuma N, Kido J. A series of dibenzofuran-based n-type exciplex host partners realizing high-efficiency and stable deep-red phosphorescent OLEDs. Chem Eur J 2019;25(30):7308–14.
[3] Chen H-W, Lee J-H, Lin B-Y, Chen S, Wu S-T. Liquid crystal display and organic light-emitting diode display: present status and future perspectives. Light Sci Appl 2018;7(3):17168.
[4] Kim J-J, Han M-K, Noh Y-Y. Flexible OLEDs and organic electronics. Semicond Sci Technol 2011;26(3):030301.
[5] Tong CC, Hwang KC. Enhancement of OLED efficiencies and high-voltage stabilities of light-emitting materials by deuteration. J Phys Chem C 2007;111(8):3490–4.
[6] Wu S, Aonuma M, Zhang Q, Huang S, Nakagawa T, Kuwabara K, et al. High-efficiency deep-blue organic light-emitting diodes based on a thermally activated delayed fluorescence emitter. J Mater Chem C 2014;2(3):421–4.
[7] Sun Y, Giebink NC, Kanno H, Ma B, Thompson ME, Forrest SR. Management of singlet and triplet excitons for efficient white organic light-emitting devices. Nature 2006;440(7086):908–12.
[8] Liu Y, Li C, Ren Z, Yan S, Bryce MR. All-organic thermally activated delayed fluorescence materials for organic light-emitting diodes. Nat Rev Mater 2018;3:18020.
[9] Godumala M, Choi S, Kim SK, Kim SW, Kwon JH, Cho MJ, et al. Highly efficient bipolar host materials towards solution-processable blue and green thermally activated delayed fluorescence organic light emitting diodes. J Mater Chem C 2018;6(37):10000–9.
[10] Hung Y-T, Chen Z-Y, Hung W-Y, Chen D-G, Wong K-T. Exciplex cohosts employing nonconjugated linked dicarbazole donors for highly efficient thermally activated delayed fluorescence-based organic light-emitting diodes. ACS Appl Mater Interfaces 2018;10(40):34435–42.
[11] Moon JS, Ahn DH, Kim SW, Lee SY, Lee JY, Kwon JH. δ-Carboline-based bipolar host materials for deep blue thermally activated delayed fluorescence OLEDs with high efficiency and low roll-off characteristic. RSC Adv 2018;8(31):17025–33.
[12] Kang JS, Hong TR, Kim HJ, Son YH, Lampande R, Kang BY, et al. High-performance bipolar host materials for blue TADF devices with excellent external quantum efficiencies. J Mater Chem C 2016;4(20):4512–20.
[13] Shin SK, Byeon SY, Han SH, Lee JY. Novel host materials based on dibenzothiophene and carbazolylcarbazole for extended lifetime in blue phosphorescent organic light-emitting diodes. Adv Optic Mater 2018;6(3):1701007.
[14] Chen W-C, Lee C-S, Tong Q-X. Blue-emitting organic electrofluorescence materials: progress and prospective. J Mater Chem C 2015;3(42):10957–63.
[15] Rajamalli P, Senthilkumar N, Gandeepan P, Ren-Wu C-C, Lin H-W, Cheng C-H. A method for reducing the singlet–triplet energy gaps of TADF materials for improving the blue OLED efficiency. ACS Appl Mater Interfaces 2016;8(40):27026–34.
[16] Wang J, Chen J, Qiao X, Alshehri SM, Ahamad T, Ma D. Simple-structured phosphorescent warm white organic light-emitting diodes with high power efficiency and low efficiency roll-off. ACS Appl Mater Interfaces 2016;8(16):10093–7.
[17] Levermore PA, Dyatkin AB, Elshenawy Z, Pang H, Silvernail JA, Krall E, et al. Phosphorescent organic light-emitting diodes for high-efficacy long-lifetime solid-state lighting. J Photon Energy 2012;2(1):1–9.
[18] Zhou D-Y, Zamani Siboni H, Wang Q, Liao L-S, Aziz H. Host to guest energy transfer mechanism in phosphorescent and fluorescent organic light-emitting devices utilizing exciplex-forming hosts. J Phys Chem C 2014;118(41):24006–12.
[19] Zhang T, Chu B, Li W, Su Z, Peng QM, Zhao B, et al. Efficient triplet application in exciplex delayed-fluorescence OLEDs using a reverse intersystem crossing mechanism based on a ΔES–T of around zero. ACS Appl Mater Interfaces 2014;6(15):11907–14.
[20] Wang F, Liu D, Li J, Ma M. Modulation of n-type units in bipolar host materials toward high-performance phosphorescent OLEDs. ACS Appl Mater Interfaces 2017;9(43):37888–97.
[21] Jeon WS, Park TJ, Kim SY, Pode R, Jang J, Kwon JH. Ideal host and guest system in phosphorescent OLEDs. Org Electron 2009;10(2):240–6.
[22] Zhu T, Van Voorhis T. Unraveling the fate of host excitons in host–guest phosphorescent organic light-emitting diodes. J Phys Chem C 2019;123(16):10311–8.
[23] Reineke S, Walzer K, Leo K. Triplet-exciton quenching in organic phosphorescent light-emitting diodes with Ir-based emitters. Phys Rev B 2007;75(12):125328.
[24] Song D, Zhao S, Luo Y, Aziz H. Causes of efficiency roll-off in phosphorescent organic light emitting devices: triplet-triplet annihilation versus triplet-polaron quenching. Appl Phys Lett 2010;97(24):243304.
[25] Reineke S, Schwartz G, Walzer K, Falke M, Leo K. Highly phosphorescent organic mixed films: the effect of aggregation on triplet-triplet annihilation. Appl Phys Lett 2009;94(16):163305.
[26] Reineke S, Schwartz G, Walzer K, Leo K. Reduced efficiency roll-off in phosphorescent organic light emitting diodes by suppression of triplet-triplet annihilation. Appl Phys Lett 2007;91(12):123508.
[27] Zhang L, van Eersel H, Bobbert PA, Coehoorn R. Clarifying the mechanism of triplet–triplet annihilation in phosphorescent organic host–guest systems: a combined experimental and simulation study. Chem Phys Lett 2016;652:142–7.
[28] Chen F-C, Yang Y, Thompson ME, Kido J. High-performance polymer light-emitting diodes doped with a red phosphorescent iridium complex. Appl Phys Lett 2002;80(13):2308–10.
[29] Sohn S, Park KH, Kwon S-K, Lee H-K, Ahn H, Jung S, et al. Preferential orientation of tetrahedral silicon-based hosts in phosphorescent organic light-emitting diodes. ACS Omega 2018;3(8):9989–96.
[30] Chen H-F, Yang S-J, Tsai Z-H, Hung W-Y, Wang T-C, Wong K-T. 1,3,5-Triazine derivatives as new electron transport–type host materials for highly efficient green phosphorescent OLEDs. J Mater Chem 2009;19(43):8112–8.
[31] Lee HL, Lee KH, Lee JY. Indoloindole as a new building block of a hole transport type host for stable operation in phosphorescent organic light-emitting diodes. J Mater Chem C 2019;7(20):5988–94.
[32] Oh CS, Lee JY, Noh CH, Kim SH. Molecular design of host materials for high power efficiency in blue phosphorescent organic light-emitting diodes doped with an imidazole ligand based triplet emitter. J Mater Chem C 2016;4(17):3792–7.
[33] Yoo SG, Jeon SK, Hwang S-H, Lee JY. A strong hole transport type host material for high quantum efficiency blue phosphorescent organic light-emitting diodes. J Ind Eng Chem 2015;32:72–6.
[34] Lee JY. Mixed-host-emitting layer for high-efficiency organic light-emitting diodes. J Inf Disp 2014;15(3):139–44.
[35] Kim SM, Yun JH, Han SH, Lee JY. A design strategy of bipolar host materials for more than 30 times extended lifetime in phosphorescent organic light-emitting diodes using benzocarbazole and quinazoline. J Mater Chem C 2017;5(35):9072–9.
[36] Gong M-S, Cha J-R, Lee CW. Synthesis and device properties of mCP analogues based on fused-ring carbazole moiety. Org Electron 2017;42:66–74.
[37] Adamovich V, Brooks J, Tamayo A, Alexander AM, Djurovich PI, D'Andrade BW, et al. High efficiency single dopant white electrophosphorescent light emitting diodes. New J Chem 2002;26(9):1171–8.
[38] Cheng T-Y, Lee J-H, Chen C-H, Chen P-H, Wang P-S, Lin C-E, et al. Carrier transport and recombination mechanism in blue phosphorescent organic light-emitting diode with hosts consisting of cabazole- and triazole-moiety. Sci Rep 2019;9(1):3654.
[39] Hung Y, Chiu T. Using carbazole-triazole derives host in blue phosphorescent OLEDs. In: Proc 2015 22nd international workshop on active-matrix flatpanel displays and devices. AM-FPD; 2015. p. 85–8.
[40] Wang Z, Liu F, Zheng X, Chen A, Xie J-f, Zhang W-x. Study on luminescence characteristics of blue OLED with phosphor-doped host-guest structure. Optoelectron Lett 2018;14(3):164–9.
[41] Lee J-H, Chen C-H, Lee P-H, Lin H-Y, Leung M-k, Chiu T-L, et al. Blue organic light-emitting diodes: current status, challenges, and future outlook. J Mater Chem C 2019;7(20):5874–88.
[42] Klubek KP, Tang CW, Rothberg LJ. Investigation of blue phosphorescent organic light-emitting diode host and dopant stability. Org Electron 2014;15(7):1312–6.
[43] Shin H, Lee J-H, Moon C-K, Huh J-S, Sim B, Kim J-J. Sky-blue phosphorescent OLEDs with 34.1% external quantum efficiency using a low refractive index electron transporting layer. Adv Mater 2016;28(24):4920–5.
[44] Cui L-S, Kim JU, Nomura H, Nakanotani H, Adachi C. Benzimidazobenzothiazole-based bipolar hosts to harvest nearly all of the excitons from blue delayed fluorescence and phosphorescent organic light-emitting diodes. Angew Chem Int Ed 2016;55(24):6864–8.
[45] Ihn S-G, Lee N, Jeon SO, Sim M, Kang H, Jung Y, et al. An alternative host material for long-lifespan blue organic light-emitting diodes using thermally activated delayed fluorescence. Adv Sci 2017;4(8):1600502.
[46] Komatsu R, Sasabe H, Seino Y, Nakao K, Kido J. Light-blue thermally activated delayed fluorescent emitters realizing a high external quantum efficiency of 25% and unprecedented low drive voltages in OLEDs. J Mater Chem C 2016;4(12):2274–8.
[47] Braveenth R, Lee H, Kim S, Raagulan K, Kim S, Kwon JH, et al. High efficiency green TADF emitters of acridine donor and triazine acceptor D–A–D structures. J Mater Chem C 2019;7(25):7672–80.
[48] Kim GW, Bae HW, Lampande R, Ko IJ, Park JH, Lee CY, et al. Highly efficient single-stack hybrid cool white OLED utilizing blue thermally activated delayed fluorescent and yellow phosphorescent emitters. Sci Rep 2018;8(1):16263.
[49] Kwong RC, Lamansky S, Thompson ME. Organic light-emitting devices based on phosphorescent hosts and Dyes. Adv Mater 2000;12(15):1134–8.
[50] Quinton C, Thiery S, Jeannin O, Tondelier D, Geffroy B, Jacques E, et al. Electron-rich 4-substituted spirobifluorenes: toward a new family of high triplet energy host materials for high-efficiency green and sky blue phosphorescent OLEDs. ACS Appl Mater Interfaces 2017;9(7):6194–206.
[51] Qiang Wang FL, Quinton Cassandre, Qu Yang-Kun, Rault-Berthelot Joëlle, Jeannin Olivier, Yang Sheng-Yi, et al. Cyril Poriel and Zuo-Quan Jiang. Evolution of pure hydrocarbon hosts: simpler structure, higher performance and universal application in RGB phosphorescent organic light emitting diodes. Chem Sci 2020;11(19):4887–94. https://doi.org/10.1039/D0SC01238F.
[52] Braveenth R, Lee H, Song M-G, Raagulan K, Park YH, Kim S, et al. Triazine-dibenzocarbazole based bipolar host materials for highly luminescent green and yellow phosphorescent organic light emitting diodes. Dyes Pigments 2019;163:607–14.
[53] Braveenth R, Bae I-J, Raagulan K, Kim S, Kim S, Kim M, et al. Dibenzothiophene-indolocarbazole-based bipolar material: host for green phosphorescent OLEDs and non-doped fluorescent emitter. Dyes Pigments 2019;162:466–74.
[54] Li W, Li J, Liu D, Wang F, Zhang S. Bipolar host materials for high-efficiency blue phosphorescent and delayed-fluorescence OLEDs. J Mater Chem C 2015;3(48):12529–38.
[55] Chatterjee T, Wong K-T. Perspective on host materials for thermally activated delayed fluorescence organic light emitting diodes. Adv Optic Mater 2019;7(1):1800565.

[56] Chaskar A, Chen H-F, Wong K-T. Bipolar host materials: a chemical approach for highly efficient electrophosphorescent devices. Adv Mater 2011;23(34):3876–95.

[57] Sun Q, Cui L-S, Xie Y-M, Liang J-J, Jiang Z-q, Liao L-s, et al. Aminoborane-based bipolar host material for blue and white-emitting electrophosphorescence devices. Org Electron 2017;48:112–7.

[58] Komatsu R, Sasabe H, Kido J. Recent progress of pyrimidine derivatives for high-performance organic light-emitting devices. J Photon Energy 2018;8(3):1–17.

[59] Maheshwaran A, Sree VG, Park H-Y, Kim H, Han SH, Lee JY, et al. High efficiency deep-blue phosphorescent organic light-emitting diodes with CIE x, y ($\leq$ 0.15) and low efficiency roll-off by employing a high triplet energy bipolar host Material. Adv Funct Mater 2018;28(36):1802945.

[60] Song W, Lee HL, Lee JY. High triplet energy exciplex hosts for deep blue phosphorescent organic light-emitting diodes. J Mater Chem C 2017;5(24):5923–9.

[61] Jeong SH, Lee JY. Dibenzofuran derivative as high triplet energy host material for high efficiency in deep blue phosphorescent organic light-emitting diodes. Org Electron 2012;13(7):1141–5.

[62] Park IS, Seo H, Tachibana H, Kim JU, Zhang J, Son SM, et al. Cyclohexane-coupled bipolar host materials with high triplet energies for organic light-emitting diodes based on thermally activated delayed fluorescence. ACS Appl Mater Interfaces 2017;9(3):2693–700.

[63] Lee DR, Hwang S-H, Jeon SK, Lee CW, Lee JY. Benzofurocarbazole and benzothienocarbazole as donors for improved quantum efficiency in blue thermally activated delayed fluorescent devices. Chem Commun 2015;51(38):8105–7.